Experimental investigation on the effects of bifurcation angle on enhanced microscale heat transfer in macro geometry

Foo, Zi Hao; Cheng, Kai Xian; Ooi, Kim Tiow

2016

Foo, Z. H., Cheng, K. X., & Ooi, K. T. (2016). Experimental investigation on the effects of bifurcation angle on enhanced microscale heat transfer in macro geometry. Proceedings of International Conference on Mechanical, Industrial and Power Engineering (1st:2016:Tokyo,Japan), 262-274.

https://hdl.handle.net/10356/89627

MIPE-419
Experimental Investigation on the Effects of Bifurcation Angle on Enhanced Microscale Heat Transfer in Macro Geometry

Zi Hao Foo [a], Kai Xian Cheng [b], Kim Tiow Ooi
School of Mechanical and Aerospace Engineering, Nanyang Technological University, Singapore
Email: zfoo002@e.ntu.edu.sg [a], kcheng003@e.ntu.edu.sg [b]

Abstract
The effectiveness of microscale heat transfer in macro geometry has been demonstrated to produce comparable heat transfer performance to that of conventional microchannels. For this research, a microchannel was created by fitting an insert with nominal diameter 19.4 mm concentrically within a hollow cylinder with inner diameter 20.0 mm, thereby producing a microchannel with an annular gap of 300 μm. Surface profiles on the insert were optimised to recover pressure loss, aiming to address the increased pumping requirements that accompany the improvement in heat transfer capabilities. A bifurcation angle was incorporated into the offset fin geometry design. The increased heat removal capability at the same pumping power and the reduction of pumping power for the same heat removal duty for three different bifurcation angles, namely 70, 75 and 80 degrees, were investigated with respect to parallel channels. The experimental study was conducted at a constant heat flux of 500 W at Reynolds number ranging from 690 to 4600. The amount of fluid in the microchannel, heat transfer area, rate of heat supplied, average channel gap size, channel length and fin height were kept constant. Experimental results successfully validated the effectiveness of bifurcation angles in the recovery of pressure loss across the microchannel. As compared to parallel channels, the 80-degrees bifurcating fins displayed the highest enhancement of the heat transfer coefficient and greatest reduction of the pumping power, which are 27% enhanced and 52% reduced respectively, at a given heat removal duty.

Keywords: Heat transfer, bifurcation, microchannel, pressure drop, Constructal theory

1. Introduction
For a microscale channel, single phase liquid flow has been shown to achieve higher convective heat transfer coefficients, thereby improving the heat transfer efficiency of the microchannel [1]. In 1981, Tuckerman and Pease introduced the microchannel heat sink for silicon integrated circuits [2]. High heat dissipation rates of up to 10000 kW m^{-2} were attained [2], a major improvement compared to conventional macroscale methods, thus sparking interest in the development, classification and implementation of microchannels. Kandlikar [3], Palm [4] and Mohammed [5] have conducted various studies and reviews on the feasibility of

microscale heat transfer and microchannels.

In 2013, Kong and Ooi [6] proposed the usage of an annular microchannel by inserting a solid cylinder with nominal diameter of 19.4 mm within a cylinder pipe with inner nominal diameter of 20.0 mm, thereby producing a microchannel with a gap size of 300 µm. This nascent technology achieved a convective heat transfer coefficient of 20.2 kW m^{-2} K^{-1} at a Reynolds number of 5300 [6], supporting the feasibility of achieving microscale heat transfer effects using macro geometries. Furthermore, due to the scale of the system, conventional machining processes can be utilised in place of the complex and costly microfabrication techniques for the manufacturing of the microchannels, nullifying any high costs of manufacturing associated with the production of conventional microchannels [7].

A study has determined that geometrical surface profiles improved the heat transfer coefficient by 100 times in comparison to plain inserts, whereas the pumping requirements were merely increased four times [1]. Using design cues from nature, Goh and Ooi explored the effectiveness of several surface profiles to enhance the heat transfer capacity of the annular microchannel [8]. Surface profiles such as the inverted fish scale profile were fabricated on the surface of the inner solid cylinder [9] and an enhancement of the overall thermal performance was observed, using both experimental and numerical approaches. The improvement of the thermo-hydrodynamic performance of the system was attributed to the re-initialisation of boundary layers and higher turbulence due to the surface profile [9]. Although the heat transfer capabilities of the annular micro-channel had been improved, it was accompanied by a greater percentage increase in pressure drop and demanded higher pumping requirements. This rendered the design to be cost ineffective and contradicted the ultimate aim of implementing microscale heat transfer in macro geometries, which was to promote energy efficiency. Thus, for the successful adoption of annular microchannels into modern heat exchangers, the surface profile must enable for a greater percentage rise in heat transfer coefficient relative to the pressure drop.

A study conducted by Rochester Institute of Technology discovered that the offset strip fin geometry provided microchannels with enhanced heat transfer capacity by restricting the fluid flow in the developing region, thereby preventing the complete formation of boundary layers, as seen in Figure 1 [1]. However, such geometry is notoriously plagued with high pressure drop and hence, for this project, a bifurcation angle was incorporated into the offset strip fin design as previous work has shown that flow bifurcation aids in the recovery of local pressure [10, 11]. Also, Constructal Law, a principle introduced in 1996, is a physical law which governs the apparent universal design in both animate and inanimate systems [12]. It states that for a finite-size flow system to persist in time, its profile must be optimised to bifurcate the liquid flow to recover pressure losses [12]. According to Constructal Law, the optimal angle of

bifurcation is 75 degrees [13].

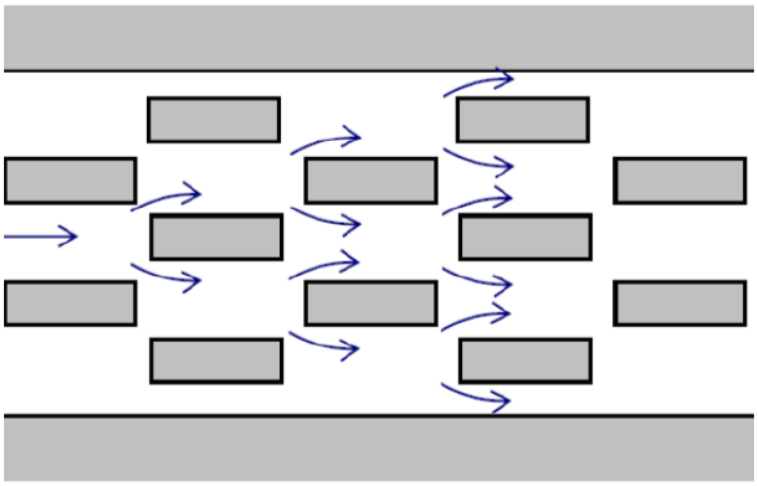

Figure 1: Fluid flow about an offset fin geometry [1]

This project experimentally investigates the effectiveness of the fin geometry surface profile in the re-initialisation of boundary layers within the microchannel, thereby raising the convective heat transfer coefficient. This project also studies the effectiveness of incorporating a bifurcation angle in the recovery of pressure loss across the microchannel. Furthermore, three different bifurcation angles, mainly 70, 75 and 80 degrees, have been incorporated into the offset fin surface profile to ascertain the applicability of Constructal Law on microchannels in macro geometries. These inserts are named Cfin-70, Cfin-75 and Cfin-80 respectively. The effects of bifurcation angles on the thermal and hydrodynamic performance of the microchannel were studied, using a parallel-fin surface profile as the reference, while keeping the heat transfer area, rate of heat supplied, average channel gap size, channel length and fin height constant.

2. Experimental Setup and Procedures

For this project, the experimental setup as shown in Figure 2 was used in conjunction with the test module. The experimental setup comprises mainly the test module, flow loop, filter, chiller, measurement devices and a data acquisition system. The flow loop comprises mainly the test loop and by-pass cum air-vent loop and distilled water was pumped out from the reservoir at a controlled temperature into the test loop. The flow rate in the test loop was regulated using the ball valve and the needle valve and measured using the Coriolis flow meter. The air-vent loop served to remove any air bubbles trapped in the flow.

The working fluid was first channeled through 40-micron tee-type filter to remove any solid impurities before entering the test loop. T-type thermocouples and pressure transducers were placed along the test loop to monitor the temperature and pressure of the flow respectively. The

parameters obtained were used for data processing.

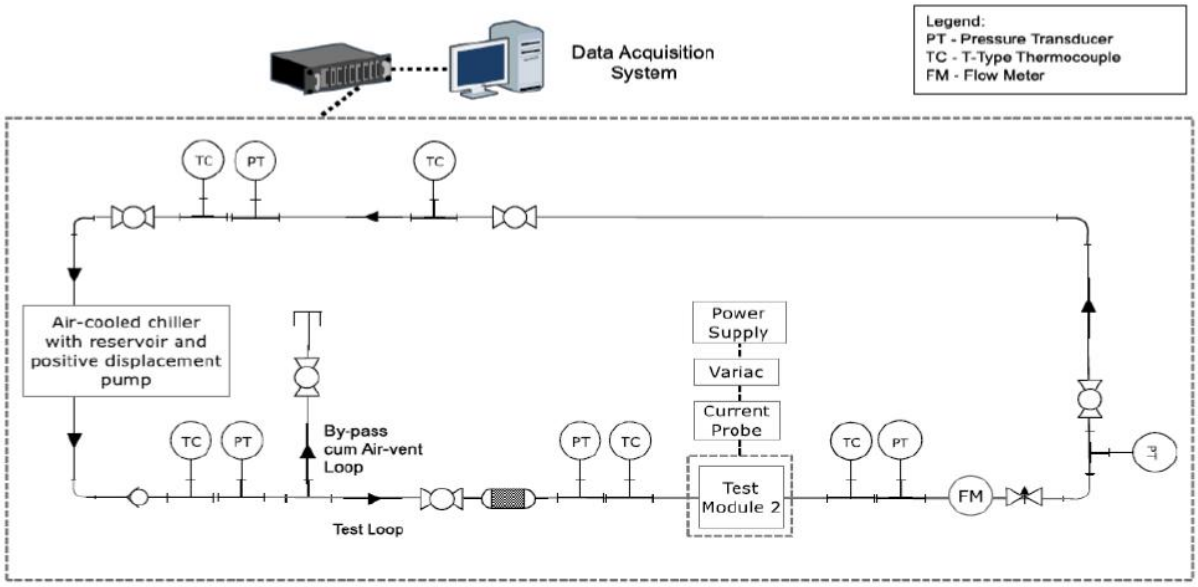

Figure 2: Experimental setup

Figure 3 shows the key conceptual design of the test module. The test module comprises two stainless steel insert holders, two polyether ether ketone (PEEK) insulation pipes, a cylindrical copper block with heater, a stainless steel insert and a MICA insulating cover. An annular microchannel was produced by placing an insert with a nominal diameter of 19.4 mm concentrically within a hollow copper coiled heater with inner diameter of 20 mm, as seen in Figure 3. Liquid flow was thus, restricted to the annular gap between the insert and the copper heater. Hence, the flow channel has a nominal gap of 0.3 mm and a length of 30 mm. The copper block with pressed on heater supplied a constant heat flux to the water within the heat transfer region and the PEEK insulation pipes and MICA insulation cover served to minimise heat loss to the surroundings.

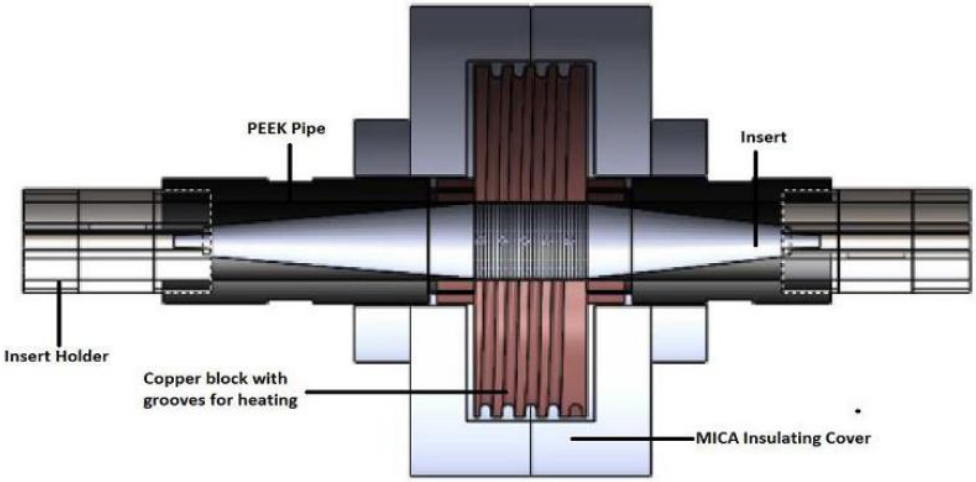

Figure 3: Key components of the test module

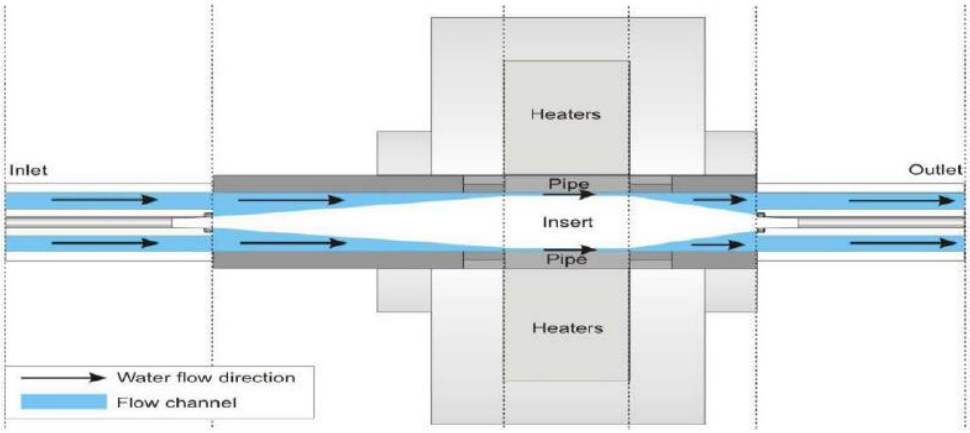

Figure 4: Cross-sectional view of test module

For this project, a total of four inserts were fabricated and investigated experimentally, namely Cfin-70, Cfin-75, Cfin-80 as well as the control insert Cfin-Parallel. Figure 5 and 6 illustrate the Cfin-parallel and Cfin-75 inserts respectively. Cfin-70, Cfin-75 and Cfin-80 each featured an offset fin geometry surface profile with bifurcation angles of 70, 75 and 80 degrees respectively. The bifurcation angles were ascertained using the ZEISS Axiovert 40M microscope to ensure conformity with design and Figure 7 shows a microscopic screenshot of Cfin-70. All the inserts had a nominal diameter of 19.4 mm in the heating region to ensure constant amount of fluid in the microchannel.

Figure 5: Cfin-75 insert

Figure 6: Cfin-Parallel insert

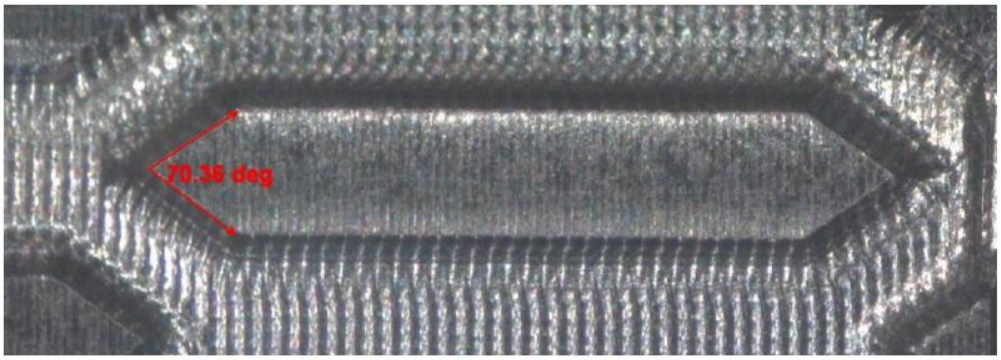

Figure 7: Microscopic screenshot using Axiovert 40M for Cfin-70

In order to obtain localised temperature at a point in the setup, J-type and T-type thermocouples were installed to acquire the required readings. Two T-type thermocouples were installed before and after the test module to acquire the temperature of the distilled water entering and leaving the test module respectively. Three other T-type thermocouples were also spread over the test loop for monitoring purposes. J-type thermocouples were installed in the test module to measure the temperature at different locations of the copper heater. Five J-type thermocouples were installed on each side of the test module to obtain readings for the surface temperature of the test module. It has a stated temperature range of -40 to 750℃, which was sufficiently able to cover the expected experimental temperature range of 25 to 500℃.

In order to obtain readings for the localised pressure at various points in the test loop, five WIKA model A-10 pressure transducers were installed within the test loop. Two of pressure transducer were placed before and after the test module in order to deduce the pressure drop across the test module while the other three were distributed over the flow loop to for monitoring purposes. The flow rate was measured by a Coriolis mass flow meter, which has a stated operating range of 0.1 to 10 L min^{-1}. A data acquisition system has been designed to acquire the output signals of the respective measuring sensors, convert them into the respectively values and transfer the finalised values into the computer system for analysis and monitoring purposes. In total, four National Instruments (NI) modules were utilised in this setup. Two NI 9208 were used to acquire data for the pressure transducer and Coriolis flowmeter and two NI 9213 were equipped to collect data for the thermocouples.

3. Results

3.1 Data Reduction

After steady state flow was achieved within the microchannel, the experiment was allowed to run continuously for 10 minutes, and the data acquired was used to tabulate the hydrodynamic and thermal dependent variables. The heat transfer coefficient, *h*, was calculated using the Newton's law of cooling shown in Equation (1). *A* is the heat transfer surface area and is kept constant at 1885 mm^2.

$$h = \frac{\dot{Q}}{A\left(T_{w,m} - T_{f,m}\right)} \tag{1}$$

The rate of heat convection, $\dot{Q}$ can be determined using the experimental readings. The temperature of the fluid at the outlet and inlet of the test module, T_{out} and T_{in} respectively, are measured using the T-type thermocouple. The mass flow rate, $\dot{m}$ was determined using the product of the temperature dependent density of the fluid and volumetric flow rate. All temperature dependent fluid properties were obtained from the National Institute of Standards and Technology (NIST) Reference Fluid and Thermodynamic and Transport Properties Database (REFPROP).

$$\dot{Q} = \dot{m} c_{p,average} \left(T_{out} - T_{in}\right) \tag{2}$$

For the computation of the mean fluid temperature, Equation (3) was employed, where the mean fluid temperature was calculated to be the average of the inlet and the outlet fluid temperature.

$$T_{f,m} = \frac{T_{in} + T_{out}}{2} \tag{3}$$

The wall temperature was deduced using the J-type thermocouples. The thermal resistance of the copper block in the radial direction due to heat conduction was taken into account and computed using Equation (4).

$$T_{w,i} = T_{r,i} - q\frac{\ln\left(d_r / d_w\right)}{2\pi L k_c} \tag{4}$$

Following which, the wall temperature was computed as the average of ten points along the wall of the copper block, as shown in Equation (5).

$$T_{w,m} = \left(\sum_{i=1}^{10} T_{w,i} \right) / 10 \tag{5}$$

The pressure drop was deduced from the pressure difference between the inlet and outlet of the test module as shown in Equation (6)

$$\Delta P = P_{in} - P_{out} \tag{6}$$

The Nusselt number and the Reynolds number was computed using Equation (7) and (8) respectively.

$$Nu = \frac{hL_c}{k_f} \tag{7}$$

$$\mathrm{Re} = \frac{\dot{m} L_c}{A_c \mu} \tag{8}$$

For an internal flow, the Reynolds and the Nusselt number are numerically related to the characteristic length (L_c) as seen in equation (7) and (8). For this experiment, the characteristic length was calculated using the derived formula shown in equation (9).

$$L_c = \frac{4A_c}{P} = \frac{4\pi(R_{out}^2 - R_{in}^2)}{2\pi(R_{out} + R_{in})} = 2(R_{out} - R_{in}) = D_{out} - D_{in} \tag{9}$$

The performance evaluation index for the two main objectives of this research, which is the increased heat removal duty for equal pumping power and the reduced pumping power per unit of heat removal were introduced by Webb [14-16]. Equation (10) evaluates the increased heat duty at a given pumping power while Equation (11) quantifies the performance of the surface profile at reducing the pumping power for a given heat removal capacity. The subscript r refers to the reference surface or the Cfin-Parallel insert for this project.

$$\frac{UA}{U_r A_r} = \frac{Nu / Nu_r}{(\Delta P / \Delta P_r)^{1/3}} \tag{10}$$

$$\frac{P}{P_r} = \frac{\Delta P / \Delta P_r}{(Nu / Nu_r)^3} \tag{11}$$

The experimental study was conducted for Reynolds number ranging 690 from to 4600 with a constant heat supply of 500 W while keeping the heat transfer area constant at 18.85 cm^2.

3.2 Experimental Results and Discussions

The variation of the heat transfer coefficient with Reynolds number for the four inserts are presented in Figure 8. The highest heat transfer coefficient obtained for this study was 36.6 kW m^{-2} K^{-1} by Cfin-80 at a Reynolds number of 4563. This is equivalent to a Nusselt number of 35.82. From Figure 8, it is explicit that all inserts with discontinuous bifurcating-fin profile attained higher heat transfer coefficient compared to Cfin-Parallel. Cfin-80 yielded the highest

heat transfer coefficient across all tested Reynolds number. Nevertheless, Cfin-70 and Cfin-75 attained close heat transfer performance at all Reynolds number. Similarly, the highest pressure drop was registered by Cfin-80 across all tested Reynolds number as illustrated by Figure 9. The pressure drop for all inserts increases with the Reynolds number, which is largely supported by classical fluid mechanics [17].

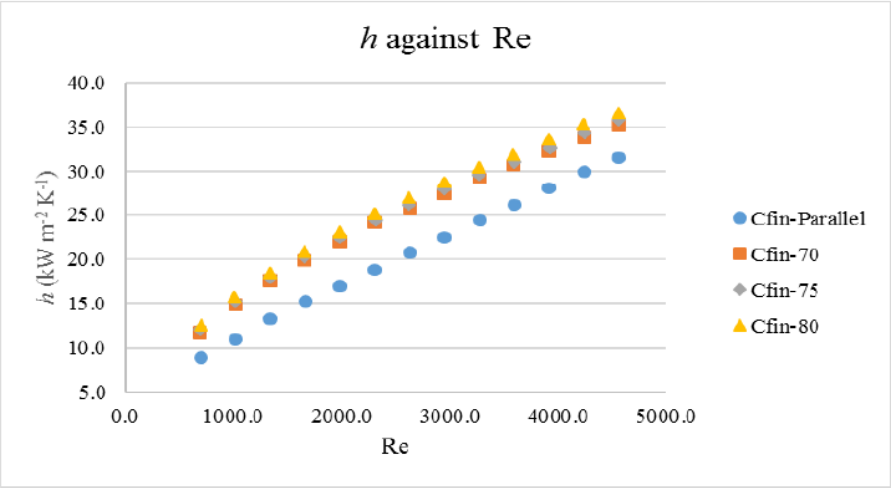

Figure 8: Heat transfer coefficient against Reynolds number

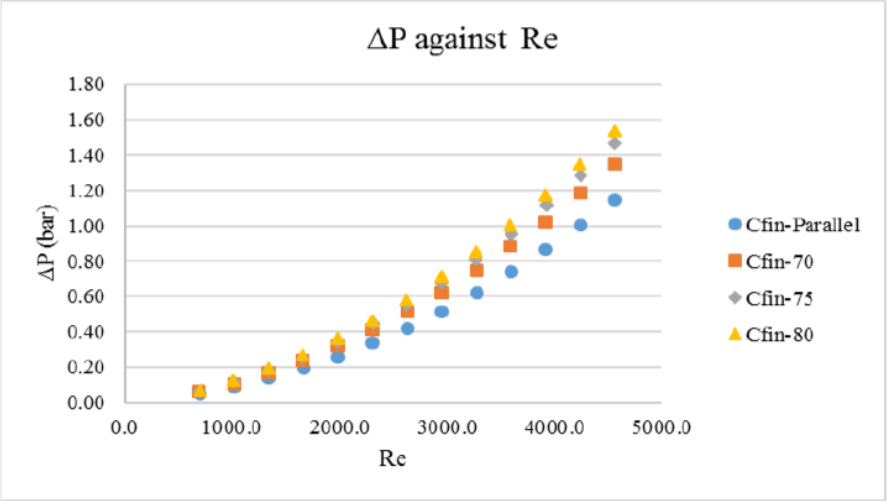

Figure 9: Pressure drop against Reynolds number

Figure 10 compares the performance of all the inserts against the Cfin-Parallel, illustrating the relative improvement in the heat removal capability at the same pumping power. The enhancement in the heat removal capability at a given pumping power of the Cfin inserts are explicit in comparison to Cfin-Parallel. The highest index registered was 1.27 by Cfin-80 at a Reynolds number of 1014, which is a 27 percent improvement relative to the parallel channels. This improvement could be attributed to varying surface height due to the offset fin, giving rise to the re-initialisation of boundary layers, thereby raising the convective heat transfer coefficient. The relative improvement of the Cfin inserts decreases with increasing Reynolds

number, where the rate of decrement of the performance index spiked between the Reynolds number of 1018 and 1339.

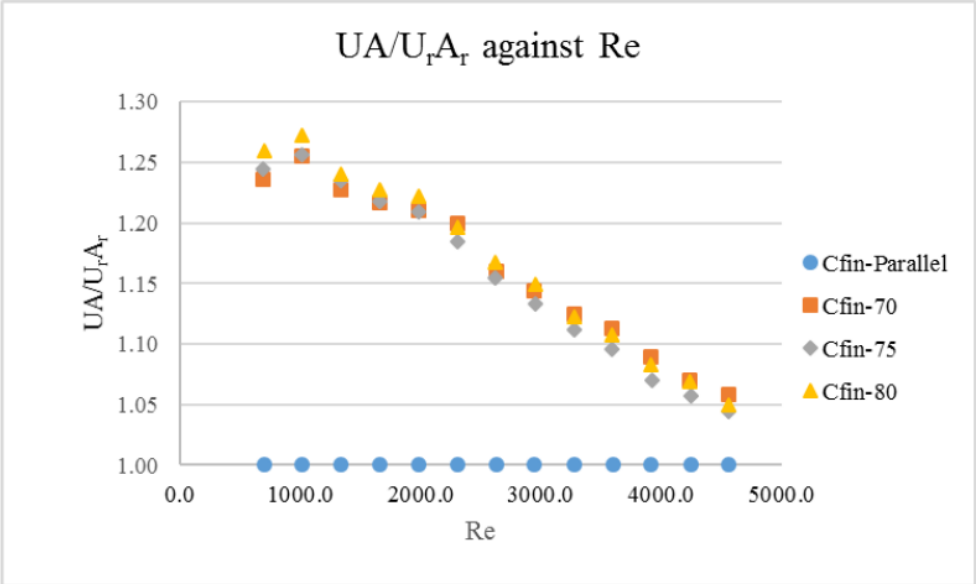

Figure 10: UA/U_rA_r against Re

Figure 11 depicts the plot of the performance index which quantifies the relative pumping power while keeping the heat removal capability of the inserts constant. The reduction of the pumping power at a constant heat removal capacity of the Cfin inserts was stark, where the performance index for all Cfin inserts relative to Cfin-Parallel is less than 1 for all tested Reynolds number. The optimum performance index was 0.486, displayed by Cfin-80 at a Reynolds number of 1014. The pressure recoveries at the bifurcation compensated the pressure drop induced by the re-initialisation of the boundary layers and the turbulence regime. The results demonstrated the effectiveness of a bifurcation angle in the recovery of pressure loss as the high pressure loss associated with the offset fin surface profile has been rectified. However, based on the relative performance of the Cfin inserts, it is worth noting that the Cfin-75 insert did not achieve the greatest reduction in the pumping power at a given heat removal capacity, which was hypothesized due to the application of Constructal law. The deviation of the experimental results from the theoretical predictions could be attributed to the lack of optimisation of the fin dimensions to cater for the operating conditions. Constructal law states that, for the fluid flow to persist, the configuration of microchannel must be optimised to provide path of lesser resistance. However, for this research, the other parameters of the offset fin surface profile were kept constant as the bifurcation angle was the subject of study.

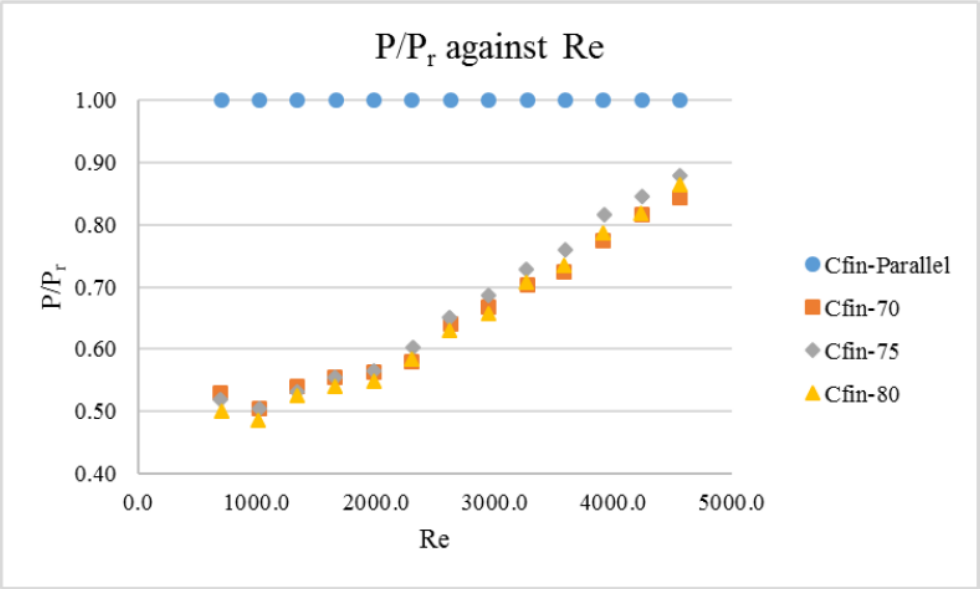

Figure 11: P/P_s against Re

In conclusion, this research demonstrated the feasibility of enhancing the thermal and hydrodynamic performance of microchannel in macro geometry using surface profiles. Experimental results showed that bifurcating offset fins performed better than parallel fins both in heat transfer capabilities and pressure drop. For a given pumping power, this project experimentally demonstrated the effectiveness of the fin geometry surface profile in raising the convective heat transfer coefficient by 27 percent at a Reynolds number of 1014, which could be attributed to the re-initialisation of boundary layers within the microchannel. Furthermore, the experimental results successfully validated the effectiveness of bifurcation angles in the recovery of pressure loss across the microchannel, where the pressure drop was reduced by 52% at a Reynolds number of 1014. The high heat transfer capacity of the offset fin geometry was coupled with a relatively lower percentage increment in pressure drop. Hence, optimisation of the geometry of the bifurcating offset fins using Constructal law should be the highlight of future works to further improve the thermal and hydrodynamic performance of the surface profile.

3.3 Acknowledgments and Legal Responsibility

The authors would like to express their gratitude to the School of Mechanical and Aerospace Engineering, Nanyang Technological University and the CN Yang Scholars Programme for their financial support in this research. They are also grateful to the technicians in the Energy Systems Laboratory and the Metrology Laboratory at the School of Mechanical and Aerospace Engineering for their technical support.

4. References

[1] Mark E. Steinke, S.G.K., *Single-phase Liquid Heat Transfer in Plain and Enhanced*

Microchannels, in *Fourth International Conference on Nanochannels, Microchannels and Minichannels* 2006: Limerick, Ireland p. 397-403.

[2] Tuckerman, D.B. and R.F.W. Pease, *High-performance heat sinking for VLSI.* IEEE Electron Device Letters, 1981. **2**(5): p. 126-129.

[3] Kandlikar, S.G., *History, Advances, and Challenges in Liquid Flow and Flow Boiling Heat Transfer in Microchannels: A Critical Review.* Journal of Heat Transfer, 2012. **134**(3): p. 034001-034001.

[4] Palm, B., *Heat Transfer in Microchannels.* Microscale Thermophysical Engineering, 2001. **5**(3): p. 155-175.

[5] Mohammed, H.A., et al., *Heat transfer and fluid flow characteristics in microchannels heat exchanger using nanofluids: A review.* Renewable and Sustainable Energy Reviews, 2011. **15**(3): p. 1502-1512.

[6] Kong, K.S. and K.T. Ooi, *A numerical and experimental investigation on microscale heat transfer effect in the combined entry region in macro geometries.* International Journal of Thermal Sciences, 2013. **68**: p. 8-19.

[7] S. V. Garimella, C.B.S., *Transport in microchannels-a critical review.* Annual review of heat transfer, 2003. **13**(1).

[8] A.L. Goh, B.H., K. T. Ooi, *Experimental Study of Nature-Inspired Enhanced Microscale Heat Transfer*, in *ASME 2016 5th International Conference on Micro/Nanoscale Heat and Mass Transfer*. 2016, ASME: Biopolis, Singapore.

[9] Goh, A.L. and K.T. Ooi, *Nature-inspired Inverted Fish Scale microscale passages for enhanced heat transfer.* International Journal of Thermal Sciences, 2016. **106**: p. 18-31.

[10] Wang, X.-Q., et al., *Flow and thermal characteristics of offset branching network.* International Journal of Thermal Sciences, 2010. **49**(2): p. 272-280.

[11] Ghaedamini, H., M.R. Salimpour, and A.S. Mujumdar, *The effect of svelteness on the bifurcation angles role in pressure drop and flow uniformity of tree-shaped microchannels.* Applied Thermal Engineering, 2011. **31**(5): p. 708-716.

[12] Bejan, A. and S. Lorente, *The constructal law and the evolution of design in nature.* Physics of Life Reviews, 2011. **8**(3): p. 209-240.

[13] A. Bejan, S.L., *Design With Construcal Law*. 1 ed. 2008: Wiley. 529.

[14] Gee, D.L. and R.L. Webb, *Forced convection heat transfer in helically rib-roughened tubes.* International Journal of Heat and Mass Transfer, 1980. **23**(8): p. 1127-1136.

[15] Webb, R.L., *Performance evaluation criteria for use of enhanced heat transfer surfaces in heat exchanger design.* International Journal of Heat and Mass Transfer, 1981. **24**(4): p. 715-726.

[16] Webb, R.L. and M.J. Scott, *A Parametric Analysis of the Performance of Internally Finned Tubes for Heat Exchanger Application.* Journal of Heat Transfer, 1980. **102**(1): p. 38-43.

[17] Bruce R. Munson, A.P.R., Theodore H. Okiishi, Wade W. Huebsch, *Fundamentals of*

Fluid Mechanics. 2013: Wiley.